Cambridge Centre for Computational Chemical Engineering

University of Cambridge

Department of Chemical Engineering

Preprint ISSN 1473 – 4273

Simulating a Homogeneous Charge Compression Ignition engine fuelled with a DEE/EtOH blend

Sebastian Mosbach[1], Markus Kraft[1], Amit N. Bhave[2],

Fabian Mauss[3], J. Hunter Mack[4], Robert W. Dibble[4]

submitted: December 8, 2005

[1] Department of Chemical Engineering
University of Cambridge
Pembroke Street
Cambridge CB2 3RA
UK

[2] Reaction Engineering Solutions Ltd.
61 Canterbury Street
Cambridge CB4 3QG
UK

[3] Division of Combustion Physics
Lund Institute of Technology
Box 118, S-221 00 Lund
Sweden

[4] Combustion Analysis Laboratory
University of California at Berkeley
Berkeley, CA 94720
USA

Preprint No. 34

c4e

Key words and phrases. HCCI, fuel blends, bio-derived fuels, stochastic reactor models.

Edited by
Cambridge Centre for Computational Chemical Engineering
Department of Chemical Engineering
University of Cambridge
Cambridge CB2 3RA
United Kingdom.

Fax: + 44 (0)1223 334796
E-Mail: c4e@cheng.cam.ac.uk
World Wide Web: http://www.cheng.cam.ac.uk/c4e/

Abstract

We numerically simulate a Homogeneous Charge Compression Ignition (HCCI) engine fuelled with a blend of ethanol and diethyl ether by means of a stochastic reactor model (SRM). A 1D CFD code is employed to calculate gas flow through the engine, whilst the SRM accounts for combustion and convective heat transfer. The results of our simulations are compared to experimental measurements obtained using a Caterpillar CAT3401 single-cylinder Diesel engine modified for HCCI operation. We consider emissions of CO, CO_2 and unburnt hydrocarbons as functions of the crank angle at 50% heat release. In addition, we establish the dependence of ignition timing, combustion duration, and emissions on the mixture ratio of the two fuel components. Good qualitative agreement is found between our computations and the available experimental data. The performed numerical simulations predict that the addition of diethyl ether to ethanol neither spreads out the combustion nor lowers light-off temperatures significantly, both in accordance with experimental observations.

Contents

1 Introduction

Homogeneous Charge Compression Ignition (HCCI) combustion provides a promising concept for reducing NO_x and particulate emissions from internal combustion engines, and achieving high thermal efficiency at the same time. However, a narrow operating window – the range of speeds and loads for stable operation – has so far prevented HCCI engines from being commercialized. Unlike spark ignition (SI) engines, where ignition timing is controlled by triggering a spark, and direct injection (DI) compression ignition (CI) engines, where ignition timing is determined by fuel injection, HCCI engines do not possess any direct control mechanism. Instead, HCCI combustion is governed mainly by chemical kinetics, which implies that alternative means of controlling combustion phasing have to be sought.

Numerous potential strategies have been an active area of research in recent years, such as exhaust gas recirculation, boosting, intake charge heating, variable valve timing, variable compression ratio, (multiple) direct injection, fuel blending/dual fuels, etc. Combinations with other operating modes are also under investigation, such as SI-HCCI-SI transitions, etc.

The motivation for using fuel blends is, among other things, to control ignition timing, to lengthen combustion duration, and to lower intake temperatures, thereby expanding the operating window. Fuel blending is made possible in part by the fuel flexibility of HCCI engines in general, and is of interest not only from the control point of view but also because of environmental considerations. Alternatives to fossil fuels, such as bio-derived fuels, are attracting more and more attention.

In [1] and [2, 3], the effects of adding dimethyl ether as an ignition improver to methane were studied experimentally as well as numerically. They also elucidated in detail the chemical mechanism of both fuels and the interaction of the elementary reactions. In [1], limitations of fuel blending are pointed out, in particular the necessity of two fuel storages and the slow response time of the mixture ratio. The latter problem might be mastered by a combination of dual fuels with port/direct injection, thereby making possible vehicular applications.

When blending fuels, the use of components with very different autoignition characteristics is desirable. The higher the octane number difference between the two fuels, the larger the attainable operating range [4]. In [5], an HCCI engine was operated with an iso-octane/n-heptane dual fuel and engine control was improved by varying the octane number. Iso-octane was replaced by ethanol in a subsequent investigation [6] to exploit a higher octane number range.

In [7], relative fuel component consumption in a blend of diethyl ether (DEE) and ethanol (EtOH) has been studied experimentally by means of a ^{14}C tracing technique. Also, numerical simulations using a single-zone model have been performed. Due to the variety of modifications and potential improvements to be investigated and the cost involved in their experimental setup and testing, computational modeling acquires an important role. Several models have been applied so far, e.g. single-zone models, multi-zone models, CFD, and probability density

function (PDF) transport models [8].

The purpose of this work is to apply a PDF-based stochastic reactor model (SRM) employed previously [9, 10, 11, 12, 13] to predict experimentally measured emissions. Furthermore, a main aim is to determine to what extent ignition timing and combustion duration can be controlled by altering the mixture ratio, and how the mixture ratio can be used to minimize combustion emissions.

This paper is structured as follows. In section 2, we briefly describe the mathematical model and sketch how it is solved numerically. In section 3, we present results of numerical simulations as well as experimental measurements of emissions of CO, CO_2, and unburnt hydrocarbons. In addition, we study the dependence of ignition timing and combustion duration as well as emissions on the mixture ratio of the two fuel blend components. Some conclusions based on the obtained results are drawn in section 4.

2 The model

2.1 The equations...

The stochastic reactor model (SRM) we employ is derived from a more general probability density function (PDF) transport model [8] and has been applied previously to HCCI engine simulation [9, 10, 11, 12, 13]. The SRM is zero-dimensional, which means that quantities are independent of space. Note, however, that the model does not assume spatial homogeneity, but rather statistical homogeneity, i.e. the statistics of turbulence – in other words the PDF – is the same everywhere. The difference is crucial, since inhomogeneities are the key to predicting combustion emissions. The quantities of interest described by the model are the mass fractions $Y_1, \ldots, Y_{N_S}$ (N_S denotes the number of chemical species) and the temperature T, which for notational convenience are combined into a vector $\psi = (\psi_1, \ldots, \psi_{N_S}, \psi_{N_S+1}) = (Y_1, \ldots, Y_{N_S}, T)$. Each of these quantities is a random variable, and their joint distribution is given by the PDF denoted by f. Once the PDF is known, mean quantities are calculated by

$$\langle \psi_j \rangle(t) = \int \psi_j f(\psi; t) \mathrm{d}\psi. \tag{1}$$

For variable density problems such as internal combustion engines it is convenient [8] to use the mass density function $\mathcal{F}(\psi; t) = \varrho(\psi, t) f(\psi; t)$. Recall that the PDF is normalized as $\int f(\psi; t) \mathrm{d}\psi = 1$, which implies for the normalization of the MDF $\int \mathcal{F}(\psi; t) \mathrm{d}\psi = \langle \varrho \rangle(t)$.

The SRM used in this work is defined by the following PDF transport equation

which describes the time evolution of the MDF.

$$\frac{\partial}{\partial t}\mathcal{F}(\psi;t) = \underbrace{-\sum_{j=1}^{N_\mathrm{S}+1}\frac{\partial}{\partial\psi_j}\big[G_j(\psi)\mathcal{F}(\psi;t)\big]}_{\text{chemical reactions, volume change}} + \underbrace{\sum_{j=1}^{N_\mathrm{S}+1}\frac{\partial}{\partial\psi_j}\Big[\frac{C_\phi}{2\tau}\big(\psi_j-\langle\psi_j\rangle\big)\mathcal{F}(\psi;t)\Big]}_{\text{IEM mixing}} - \\ \underbrace{-\frac{\dot{V}}{V}\mathcal{F}(\psi;t)}_{\text{piston movement}} \underbrace{-\frac{1}{h}\big[U(\psi_{N_\mathrm{S}+1}+h)\mathcal{F}(\psi_1,\ldots,\psi_{N_\mathrm{S}},\psi_{N_\mathrm{S}+1}+h;t)-U(\psi_{N_\mathrm{S}+1})\mathcal{F}(\psi;t)\big]}_{\text{convective heat transfer}} \tag{2}$$

The terms on the right hand side represent the various physical processes taken into account by the model, i.e. chemical kinetics, turbulent mixing, piston movement, and convective heat transfer.

The chemical reactions and their heat release including temperature change due to compression and expansion are summarized in the function $G(\psi)$ defined by

$$\begin{aligned} G_j(\psi) &= \frac{M_j\dot{\omega}_j}{\varrho}, \qquad j=1,\ldots,N_\mathrm{S} \\ G_{N_\mathrm{S}+1}(\psi) &= -\frac{1}{c_V\varrho}\sum_{i=1}^{N_\mathrm{S}+1}e_iM_i\dot{\omega}_i - \frac{p}{c_Vm}\frac{\mathrm{d}V}{\mathrm{d}t}, \end{aligned} \tag{3}$$

which generates the time evolution of the mass fractions and the temperature. Here, M_j denotes the molar mass, $\dot{\omega}_j$ the molar production rate, and e_j the specific internal energy of the j^{th} species. ϱ denotes the mass density, c_V the specific heat capacity at constant volume, m the total mass, and V the instantaneous cylinder volume.

For the description of turbulent mixing we use the Interaction by Exchange with the Mean (IEM) model, in which all scalars relax exponentially to their mean value. The mixing intensity is given by $C_\phi/2\tau$, where we set $C_\phi = 2$ as recommended in [8], and τ denotes the characteristic mixing time.

For convective heat transfer we employ a model using Woschni's heat transfer coefficient h_g [14],

$$U(T) = -\frac{h_gA}{c_Vm}(T-T_\mathrm{W}), \tag{4}$$

where A is the available heat transfer area, and T_W is the cylinder wall temperature (assumed to be uniform).

2.2 . . . and their solution.

The PDF transport equation (2) describing the SRM together with (3) and (4) is solved by a Monte Carlo particle method, in which the PDF is approximated by a notional ensemble of N_par stochastic particles. These particles are not to be confused with physical atoms or molecules, fluid parcels, or zones in a multi-zone

approach. They carry no geometric or spatial information whatsoever, but as an ensemble constitute a statistical representation of the PDF. Each particle carries with it only mass fractions and temperature, i.e. $\psi^{(i)} = (\psi_1^{(i)}, \ldots, \psi_{N_\mathrm{S}}^{(i)}, \psi_{N_\mathrm{S}+1}^{(i)}) = (Y_1^{(i)}, \ldots, Y_{N_\mathrm{S}}^{(i)}, T^{(i)})$. We employ throughout the convention that subscript indices label species, whereas superscript indices in parentheses label particles. The PDF is then represented by

$$f(\psi; t) = \frac{1}{N_\mathrm{par}} \sum_{i=1}^{N_\mathrm{par}} \delta\big(\psi - \psi^{(i)}(t)\big). \tag{5}$$

Inserting Eqn. (5) into (1) yields as approximation of mean quantities

$$\langle \psi_j \rangle(t) = \frac{1}{N_\mathrm{par}} \sum_{i=1}^{N_\mathrm{par}} \psi_j^{(i)}(t).$$

In order to make Eqn. (2) accessible to implementation, an operator splitting technique (see for example [15] or [8]) is used so that each of the terms can be treated separately. Standard techniques are applied to each of these terms, except for heat transfer, which is modelled as stochastic jump process. In a heat transfer step, particles are chosen at random, whose temperature is then adjusted according to

$$T^{(i)} \mapsto T^{(i)} - \frac{T^{(i)} - T_\mathrm{W}}{C_\mathrm{h}}, \tag{6}$$

where C_h is a constant controlling the magnitude of the temperature fluctuations.

3 Numerical study

Table 1: *Caterpillar CAT3401 engine specification and experimental operating conditions.*

Parameter	Value
Bore	137.2 mm
Stroke	165.1 mm
Connecting rod length	261.6 mm
Displaced volume	2.44 l
Compression ratio	16.25
Intake valve opening	3 CAD ATDC
Intake valve closing	10 CAD BBDC
Exhaust valve opening	19 CAD BBDC
Exhaust valve closing	7 CAD BTDC
Speed	1800 RPM
Fuel	EtOH/DEE blend
Fuel/air equiv. ratio	0.3-0.4
Intake pressure	1.7 bar

In this section we report on numerical simulations carried out and compare their results to experimental measurements. Our FORTRAN implementation of the SRM described in the previous section has been coupled to the commercial 1D CFD code GT-Power, so that full cycle simulations can be performed. The CFD code calculates the gas flow through the engine, whilst the SRM accounts for combustion, turbulent mixing, and convective heat transfer during the closed-volume part of the cycle (i.e. from IVC to EVO). The cylinder charge is assumed to be homogeneous in composition and temperature at IVC. The chemical kinetics are solved using the Sandia CHEMKIN II package [16] and a chemical mechanism [17] containing 112 species and 484 reversible reactions, which covers both DEE and EtOH chemistry.

Experiments were conducted using a Caterpillar CAT3401 single-cylinder Diesel engine modified for port-injected HCCI operation. Table 1 lists some of the most important parameters. For details on the experimental setup see [7].

3.1 Model calibration

Before the model can be used to predict quantities of interest, each of its parameters needs to be fixed. Many of these, such as the compression ratio for instance, are determined by the engine specification or the particular operating condition chosen (see Table 1). We employed precisely the values given in Table 1, except for the intake pressure which we fixed at 1.18 bar. Some parameters are experimentally more difficult to quantify, such as the mixing time τ, or specific to our model, such as the constant C_h which governs temperature fluctuations (see Eqn. 6), which often means there is no data available. There are also purely numerical parameters, such as the particle number N_par most importantly, and one has to make sure that predictions do not depend on any of the numerical parameters. Once model parameters have been determined, they are kept constant for the remainder of the study.

For calibration, we used experimentally measured pressure profiles at known operating conditions using pure EtOH as fuel. Model parameters for which there is no information available are adjusted such that simulated profiles coincide with experimental ones as accurately as possible. Due to the considerable number of model parameters, many parameter sets exist (in fact a submanifold of the parameter space) which fit a given set of experimental profiles. For this reason it is helpful for the modeler to have available several curves for which only one parameter varies. Figure 1 shows two simulated pressure curves which agree well with the experimentally measured profiles. Note that the only parameter which is different for the two cases is the inlet temperature, all other parameters are identical.

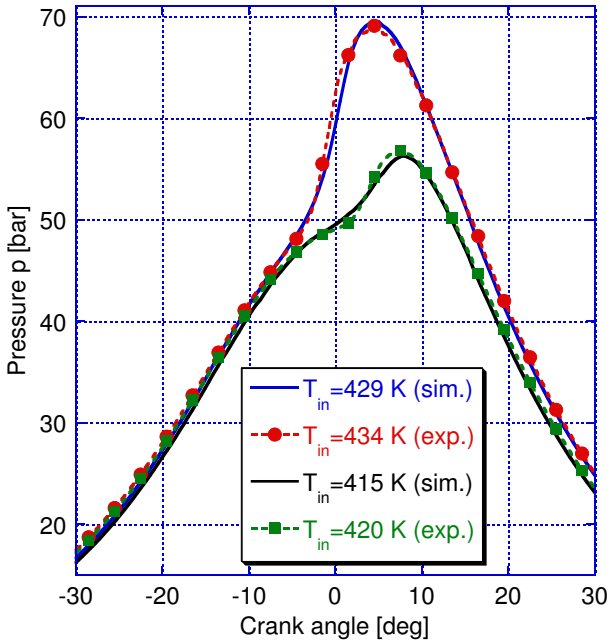

Figure 1: Calibration of model parameters by means of in-cylinder pressure profiles (for pure EtOH).

As a result of these initial studies, we opted for $C_\mathrm{h} = 20$, a cylinder wall temperature of $T_\mathrm{W} = 400$ K, and a mixing time of $\tau = 20$ ms. We decided to use $N_\mathrm{par} = 100$ particles throughout, since little change in predicted quantities could be observed for higher values. Furthermore, we performed multiple cycle simulations in order to establish that the simulation had reached steady state. During these tests we found in addition that the influence of 5% trapped residual gas (internal exhaust gas recirculation) on CA50 and emissions was small (i.e. both chemically and thermally).

3.2 Emissions

The calibrated model was used to predict the dependence of emissions of CO, CO_2, and unburnt hydrocarbons (HC) on CA50, which is defined as the crank angle at which 50% of the cumulative heat release occurs. Experimentally as well as in our simulations, CA50 was varied by altering the inlet temperature, but the fuel/air equivalence ratio Φ was kept constant at a value of 0.4.

In order to describe the fuel composition, we introduce the quantity Λ which denotes the liquid volume fraction of DEE used for preparing the DEE/EtOH mixture, i.e. $\Lambda = V_\mathrm{DEE}/(V_\mathrm{DEE} + V_\mathrm{EtOH})$. For example, $\Lambda = 25\%$ means 250 ml of DEE for every 750 ml of EtOH. $\Lambda = 0$ corresponds to pure EtOH, $\Lambda = 1$ to pure DEE. This capital Λ is not to be confused with the air/fuel equivalence ratio $\lambda = 1/\Phi$. Note that in a first approximation, the mass fraction of DEE in the fuel mixture roughly equals Λ, with at most a few percent deviation.

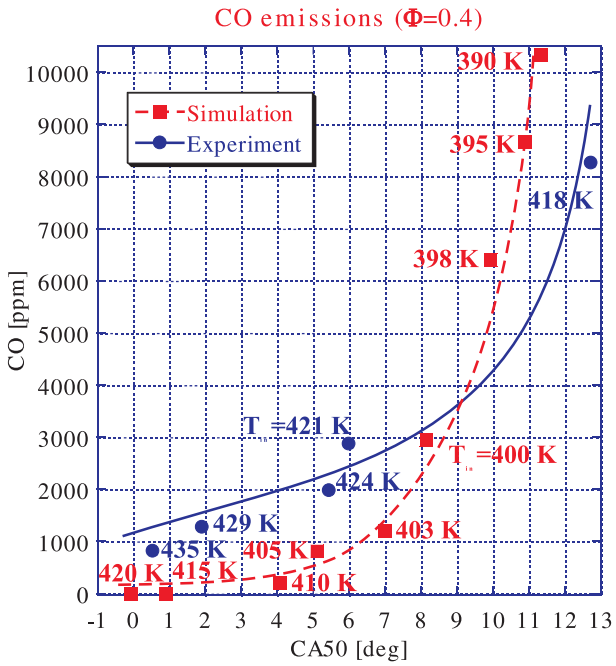

Figure 2: Emissions of CO as function of CA50 (for $\Lambda = 25\%$) with inlet temperatures.

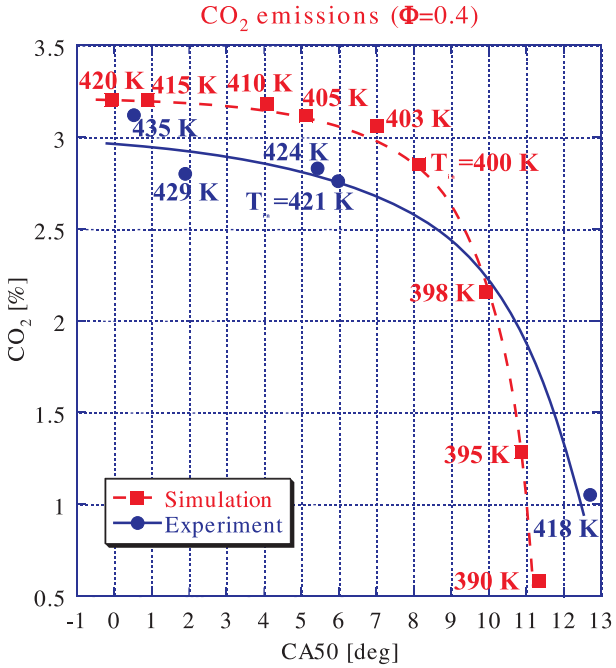

Figure 3: Emissions of CO_2 as function of CA50 (for $\Lambda = 25\%$) with inlet temperatures.

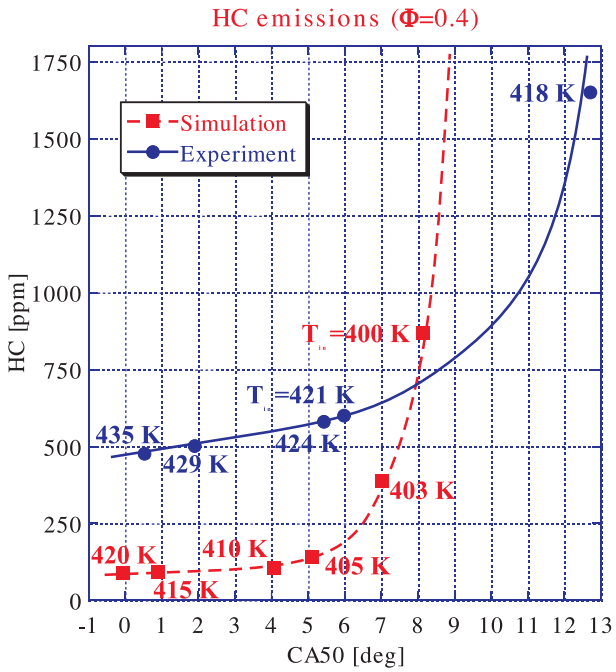

Figure 4: Emissions of unburnt hydrocarbons as function of CA50 (for $\Lambda = 25\%$) with inlet temperatures.

Figures 2, 3, and 4 show emissions (mole fractions) of CO, CO_2, and unburnt hydrocarbons respectively as functions of CA50 for $\Lambda = 25\%$. Both experimental measurements and simulation results are shown. In all three cases, the general trend is correctly predicted with satisfactory agreement. Furthermore, the following observations can be made. For large values of CA50 (roughly greater than 8 CAD), CO (Fig. 2) and unburnt hydrocarbons emissions (Fig. 4) are rising sharply, whereas CO_2 (Fig. 3) emissions are dropping. This agrees with expectation since for increasing values of CA50 combustion proceeds less and less to completion. We attribute the fact that this occurs earlier numerically than experimentally to the experimental (and computational) uncertainty associated to CA50 of the order of a few degrees. For values of CA50 smaller than 8 CAD, CO (Fig. 2) and unburnt HC emissions (Fig. 4) are clearly underpredicted. We believe this is due to the fact that the model takes into account neither crevices nor a thermal boundary layer, both of which are significantly colder than the bulk and hence contribute substantially to CO and HC emissions.

Since charge inhomogeneities (particularly in temperature) are crucial for correctly predicting emissions, we have tested the dependence of emissions on the mixing model by replacing IEM with the Euclidian Minimal Spanning Tree (EMST) model [18]. In contrast to IEM, the EMST model takes into account localness in composition space, which means that a stochastic particle mixes preferentially with particles which are close to it in composition. We found only minor differences between the two models. This can be explained by the fact that inhomogeneities are mild compared to non-premixed situations (like Diesel engines or diffusion flames), where it has been shown that the mixing model can drastically affect calculation

results [19, 20].

3.3 Mixture ratio of the fuel components

In this subsection we study numerically the dependence of ignition timing, combustion duration, and CO, CO_2, and HC emissions on the mixture ratio Λ of the two fuel components DEE and EtOH. The prime quantity to be controlled by the mixture ratio in order to achieve stable engine operation is the ignition timing.

Figure 5 depicts the dependence of CA50 on the mixture ratio of the fuel components. In this figure and all the following ones, three curves each at constant inlet temperature are shown, one at $T_{\rm in} = 410$ K at constant fuel/air ratio $Y_{\rm f}/Y_{\rm a} \approx 0.043$ (corresponding to $\Phi = 0.4$), one at $T_{\rm in} = 420$ K at constant $Y_{\rm f}/Y_{\rm a}$, and one at again $T_{\rm in} = 410$ K but constant Φ. Raising the temperature by 10 K advances ignition by 3 to 4 CAD. At constant $Y_{\rm f}/Y_{\rm a}$, Φ varies by about 20% for Λ between zero and unity because of the different stoichiometry of the two fuel components. In any case, it is evident that the more DEE is added to EtOH the earlier the mixture ignites, which is to be expected, since DEE is known to be more reactive than EtOH.

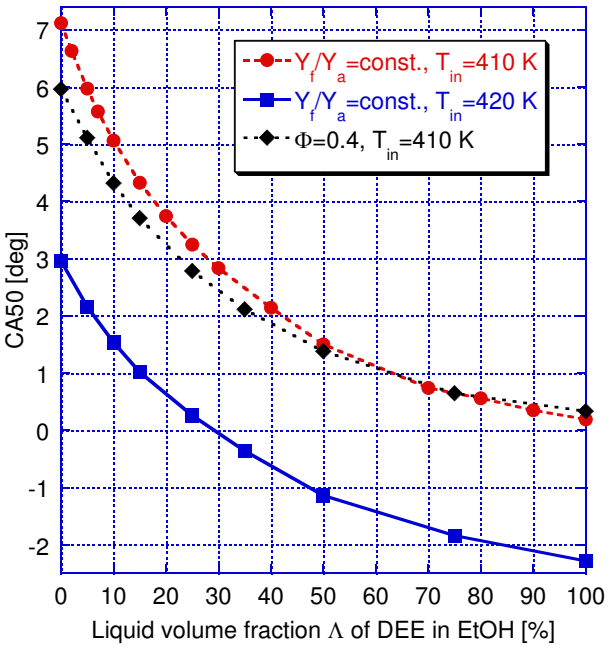

Figure 5: Simulated crank angle at 50% heat release (CA50) as function of the DEE/EtOH mixture ratio Λ.

Figure 6 shows the combustion duration as function of the mixture ratio Λ. We define combustion duration as CA90−CA10, that is, the difference between the crank angles at 90% and 10% cumulative heat release. As expected, raising the temperature reduces combustion duration appreciably, by between 1 and 4 CAD. In contrast to ignition timing, for combustion duration it does make a difference

whether the fuel/air ratio or the fuel/air equivalence ratio Φ is kept constant. In further tests we established that ignition timing and combustion duration are both much more sensitive to changes in inlet temperature than to changes in Φ.

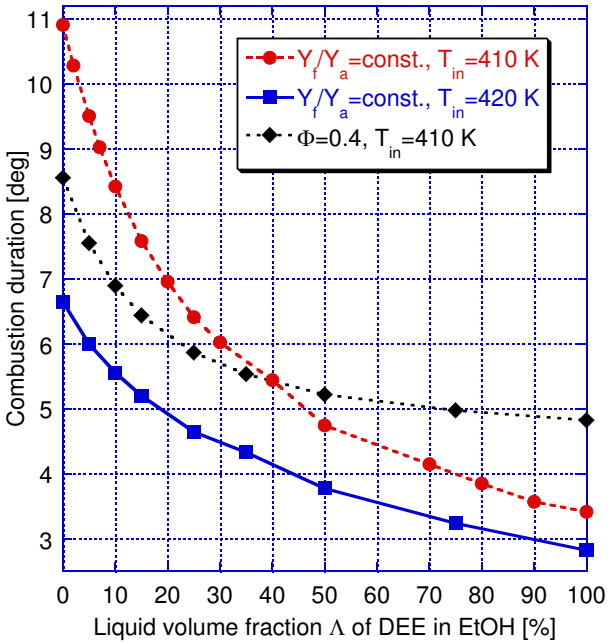

Figure 6: Simulated combustion duration (CA90−CA10) as function of the DEE/EtOH mixture ratio Λ.

Figures 7, 8, and 9 display emissions of CO, CO_2, and unburnt HC respectively as functions of the mixture ratio Λ. Concerning CO emissions (Fig. 7), all three curves reflect to some extent the variation of CA50 with Λ (cf. Figs. 5 and 2). Nonetheless, one can conclude that replacing some EtOH with DEE does improve ignitability of the mixture. Also, as expected, raising the temperature assists combustion and hence promotes consumption of CO. For the CO_2 emissions curves shown in Fig. 8, CA50 is practically constant (cf. Figs. 5 and 3). However, in this case maintaining $Y_\mathrm{f}/Y_\mathrm{a}$ can be quite misleading in the sense that it appears to suggest that a higher proportion of DEE increases CO_2 emissions. This is put into perspective by the curve for constant Φ, which also demonstrates that introducing a small fraction of DEE (as with CO, Fig. 7) helps combustion to proceed towards completion. Hydrocarbon emissions (Fig. 9) once again show that for sufficiently low temperatures small quantities of DEE can induce light-off. Whether $Y_\mathrm{f}/Y_\mathrm{a}$ or Φ is kept constant seems to be irrelevant (at least in the considered temperature range) for higher values of Λ, in contrast to CO_2 (Fig. 8). Note, however, that for small values of Λ, there is also some variation of CA50 with Λ involved, such as the large values of HC emissions for small Λ at $Y_\mathrm{f}/Y_\mathrm{a}$ =const., $T_\mathrm{in} = 410$ K (cf. Figs. 5 and 4).

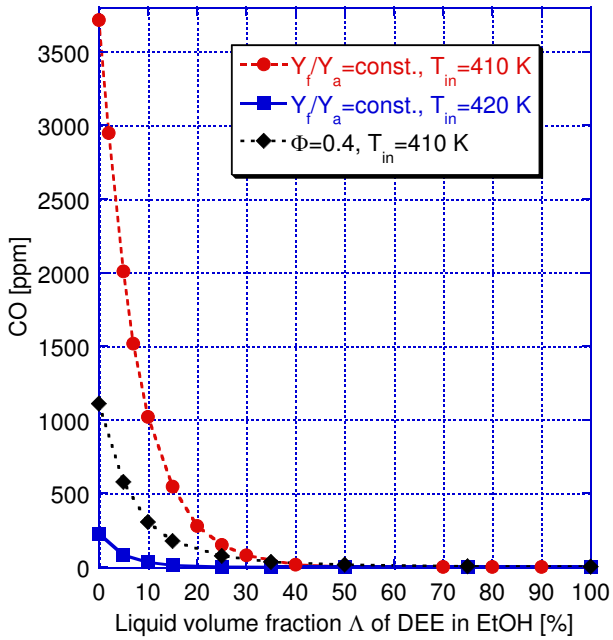

Figure 7: Simulated emissions of CO as function of the DEE/EtOH mixture ratio Λ.

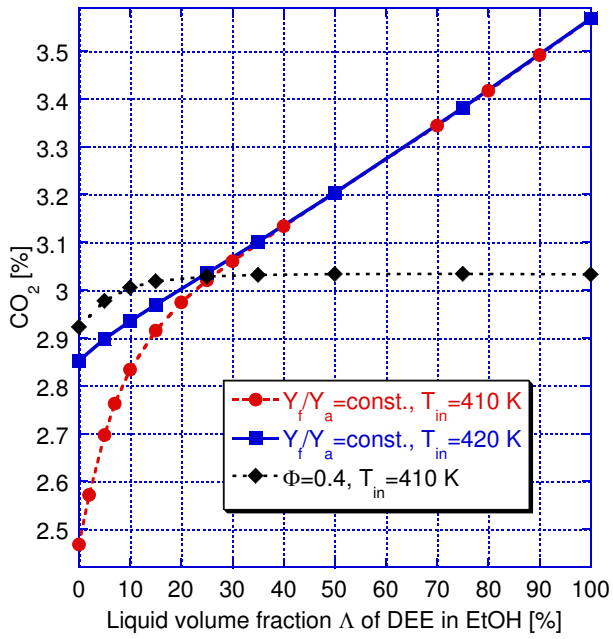

Figure 8: Simulated emissions of CO_2 as function of the DEE/EtOH mixture ratio Λ.

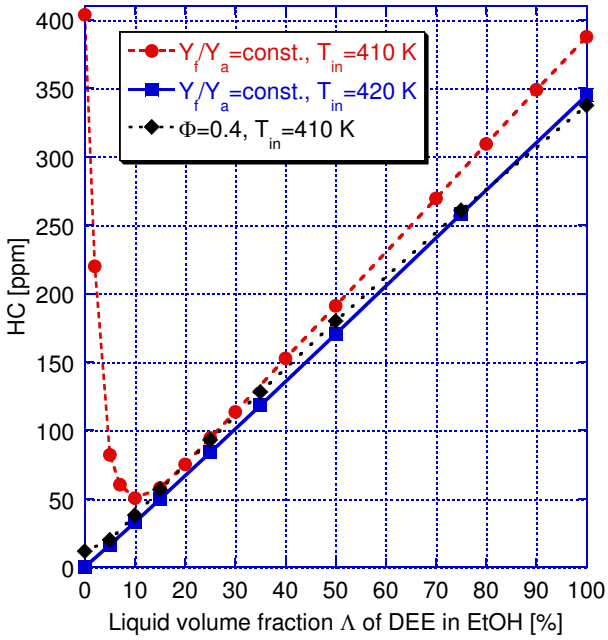

Figure 9: Simulated emissions of unburnt hydrocarbons as function of the DEE/EtOH mixture ratio Λ.

All the diagrams in this subsection indicate that adding relatively small quantities of DEE (up to about 30%) has relatively large effects, whereas increasing Λ beyond 30% has comparatively little impact. The emissions diagrams (Figs. 7, 8, and 9) have in common that both fuel/air ratio and inlet temperature can have significant influence. However, under the conditions studied, for $\Lambda \geqslant 30\%$ emissions seem almost independent of the inlet temperature, but can be very sensitive for $\Lambda < 30\%$.

Based on Figs. 7 and 9, it is legitimate to say that adding DEE to EtOH lowers light-off temperatures, as a consequence of the greater reactivity of DEE.

Furthermore, we considered the time dependence of the fuel component consumption. As noted in [7], DEE is consumed slightly earlier (in our tests by less than 3 CAD), but this exhibits little dependence on the mixture ratio.

4 Conclusions

We have performed numerical simulations of an HCCI engine fuelled with a blend of EtOH and DEE using a stochastic reactor model (SRM). We compared the results of our simulations to experimental measurements obtained using a Caterpillar CAT3401 single-cylinder Diesel engine modified for HCCI operation. We studied emissions of CO, CO_2 and unburnt HC as functions of the crank angle at 50% heat release. Not only were the general trends correctly predicted, but also reasonable qualitative agreement with experiments could be achieved. However, the model

needs to be extended to include crevices and/or a thermal boundary layer for further improvement of the calculation results. Additionally, in order to investigate the potential of DEE/EtOH blending for expanding the HCCI operating window, we established the dependence of ignition timing, combustion duration, and CO, CO_2, and HC emissions on the mixture ratio of the two fuel components. We found that several of these quantities under certain conditions are quite sensitive with respect to intake temperature. The performed numerical simulations predict that the addition of DEE to EtOH accelerates combustion as a consequence of the greater ignitability of DEE. Ignition timing and combustion duration can be controlled to some extent by adjusting the mixture ratio of the fuel components, but this is simply due to the different reactivity and consequently the different light-off temperatures of DEE and EtOH. However, there is no indication of a non-trivial interaction between the two reaction mechanisms, in contrast to what has been found for DME/methane mixtures [1, 2, 3].

Acknowledgements

Funding from the EPSRC (UK), grant number GR/R85662/01, is gratefully acknowledged. The authors thank H. Curran for providing the chemical mechanism.

References

[1] M. Konno and Z. Chen. Ignition mechanisms of HCCI combustion process fueled with methane/DME composite fuel. SAE Paper No. 2005-01-0182, 2005.

[2] M. Yao, Z. Zheng, Z. Chen, and B. Zhang. Experimental study on HCCI combustion of dimethyl ether (DME)/methanol dual fuel. SAE Paper No. 2004-01-2993, 2004.

[3] M. Yao and J. Qin. Simulating the homogeneous charge compression ignition process using a detailed kinetic model for dimethyl ether (DME) and methane dual fuel. SAE Paper No. 2004-01-2951, 2004.

[4] F. Zhao. HCCI control and operating range extension. In *Homogeneous Charge Compression Ignition (HCCI) Engines: Key Research & Development Issues*, SAE Publication PT-94, pages 325–348, March 2003.

[5] J. O. Olsson, O. Erlandsson, and B. Johansson. Experiments and simulation of a six-cylinder Homogeneous Charge Compression Ignition (HCCI) engine. SAE Paper No. 2000-01-2867, 2000.

[6] J. O. Olsson, P. Tunestål, G. Haraldsson, and B. Johansson. A turbocharged dual fuel HCCI engine. SAE Paper No. 2001-01-1896, 2001.

[7] J. H. Mack, D. L. Flowers, B. A. Buchholz, and R. W. Dibble. Investigation of HCCI combustion of diethyl ether and ethanol mixtures using carbon 14 tracing and numerical simulations. *Proc. Combust. Inst.*, 30:2693–2700, 2005.

[8] S. B. Pope. PDF methods for turbulent reactive flows. *Prog. Energy Combust. Sci.*, 11:119–192, 1985.

[9] M. Kraft, P. Maigaard, F. Mauss, M. Christensen, and B. Johansson. Investigation of combustion emissions in a HCCI engine – measurements and a new computational model. *Proc. Combust. Inst.*, 28:1195–1201, 2002.

[10] P. Maigaard, F. Mauss, and M. Kraft. Homogeneous Charge Compression Ignition engine: A simulation study on the effects of inhomogeneities. *ASME Journal of Engineering for Gas Turbines and Power*, 125(2):466–471, 2003.

[11] A. Bhave, M. Balthasar, M. Kraft, and F. Mauss. Analysis of a natural gas fuelled Homogeneous Charge Compression Ignition engine with exhaust gas recirculation using a stochastic reactor model. *Int. J. Engine Research*, 5(1):93–104, 2004.

[12] A. Bhave, M. Kraft, F. Mauss, A. Oakley, and H. Zhao. Evaluating the EGR-AFR operating range of a HCCI engine. SAE Paper No. 2005-01-0161, 2005.

[13] A. Bhave, M. Kraft, L. Montorsi, and F. Mauss. Modelling a dual-fuelled multi-cylinder HCCI engine using a PDF-based engine cycle simulator. SAE Paper No. 2004-01-0561, 2004.

[14] J. B. Heywood. *Internal Combustion Engine Fundamentals*. McGraw-Hill, New York, 1988.

[15] G. Strang. On the construction and comparison of difference schemes. *SIAM J. Numer. Anal.*, 5(3):506–517, 1968.

[16] R. J. Kee, F. M. Rupley, and J. A. Miller. CHEMKIN-II: A FORTRAN chemical kinetics package for the analysis of gas-phase chemical kinetics. Technical Report SAND89-8009, Sandia National Laboratories, 1993.

[17] H. J. Curran. Reaction mechanism for oxidation of diethyl ether, 2003. (to be published).

[18] S. Subramaniam and S. B. Pope. A mixing model for turbulent reactive flows based on Euclidean minimum spanning trees. *Combust. Flame*, 115:487–514, 1998.

[19] S. Subramaniam and S. B. Pope. Comparison of mixing model performance for nonpremixed turbulent reactive flow. *Combust. Flame*, 117:732–754, 1999.

[20] Z. Ren and S. B. Pope. An investigation of the performance of turbulent mixing models. *Combust. Flame*, 136:208–216, 2004.